Geomorphology 441 (2023) 108910

Contents lists available at ScienceDirect

Geomorphology

journal homepage: www.journals.elsevier.com/geomorphology

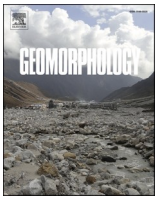

Internal structure of an active landslide based on ERT and DP data: New insights from the Hofermühle landslide observatory in Lower Austria

Julia Luhn [a,*], Margherita J. Stumvoll-Schmaltz [b], Adrián Flores Orozco [c], Thomas Glade [a]

[a] Department of Geography and Regional Research – University of Vienna, Vienna, Austria
[b] Berchtesgaden National Park, Berchtesgaden, Germany
[c] Research Unit of Geophysics, Department of Geodesy and Geoinformation, TU-Wien, Vienna, Austria

ARTICLE INFO

Keywords:
Landslide sub-surface investigation
Complex landslide
Electrical resistivity tomography (ERT)
Flysch Zone of Lower Austria

ABSTRACT

Slopes with clay-rich, deeply weathered soils, such as those present in the Flysch Zone of Lower Austria, are prone to landslide processes. Even though generally being of low magnitude and velocity, they can cause substantial economic losses and threaten settlements as well as infrastructure. Previous studies have demonstrated the importance of sub-surface information to further increase our understanding on landslide processes and triggers in different areas as well as to support any decision makers to determine any appropriate landslide mitigation measures. The combination of direct and indirect methods thereby has proven to be an adequate methodology, yet case studies are still needed to develop a universal strategy for the investigation of clay-rich landslides. In this study, we applied Electrical Resistivity Tomography (ERT) and Dynamic Probing Medium (DPM) to further investigate the complex Hofermühle landslide in the Flysch Zone of Lower Austria in order to improve our knowledge on sub-surface conditions. The focus is on the initially activated main landslide area, which has already formed earth-flow-like processes in the past. The methodology facilitated a representative characterization of the sub-surface. We were able to approximate the geometry and depth of slip surfaces, as well as the transition to bedrock, allowing us to delimit those parts of the slope which are likely to fail and, respectively be re-activated in the future. The results show that a range of thicknesses can be found in the investigated part of the Hofermühle landslide. In particular, near the surface, which has been altered by creep displacement and also by anthropogenic alteration, the resistivity is more variable compared to deeper, presumably less disturbed, layers. Furthermore, it is assumed that clay particles are transported with the surface runoff and deposited in the surroundings of the drainage channels, resulting in lower resistivity values and higher saturation at this locations. The location of the slip surface is interpreted to be on the surface of the bedrock, where there is a highly disturbed, clay-rich mass with no interbedded layers. Layers with lower resistivity directly above the bedrock indicate weathered material and remolding of materials during creep.

1. Introduction

Worldwide, landslides cause fatalities and increasing economic losses (Crozier and Glade, 2005; Bell et al., 2006; Bell, 2007; Rezaei et al., 2018; Khan et al., 2021). Landslide prone mountainous areas become increasingly inhabited (Rezaei et al., 2018; Ehrlich et al., 2021) resulting in frequently affected settlements, infrastructures and people. Hereby, the knowledge about the potentially initiated landslide mass is of major importance for all involved stakeholders. There are numerous landslide triggering mechanisms including heavy and long-lasting precipitation, volcanic activity, earthquakes, and human activity (Crozier and Glade, 2005; Rezaei et al., 2018; Imani et al., 2021; Khan et al., 2021).

In the regional state of Lower Austria, approximately 50 % of all municipalities are affected by landslides (Glade et al., 2012). Up until 2008, about 2000 damaging landslides were recorded in the building ground register alone (Glade et al., 2012). Because landslides in Lower Austria pose a risk to infrastructure and economic losses occur repeatedly, the interest of local authorities in preventing damage is high (Marr et al., 2023). Landslide processes are characterized by shallow or deep seated (earth or debris) slides (for definitions refer to Cruden and Varnes, 1996, Dikau et al., 1996, Hungr et al., 2013) which occur predominantly in the Flysch Zone (Schwenk, 1992, Petschko et al. 2016).

* Corresponding author at: Holochergasse 33/9, 1150 Wien, Austria.
E-mail addresses: julia.luhn@posteo.de, a11709932@unet.univie.ac.at (J. Luhn).

https://doi.org/10.1016/j.geomorph.2023.108910
Received 16 June 2023; Received in revised form 9 September 2023; Accepted 10 September 2023
Available online 14 September 2023

Although this geological zone covers only 9 % of the area of Lower Austria, most landslides were recorded here, which is due to the fact that it is particularly prone to sliding due to its inherent lithological characteristics – inter alia the high silt and clay contents of the deeply weathered soils (Schwenk, 1992; Bell et al., 2011). Anis et al. (2019) found that plasticity increases with clay content due to decreased cohesion and shear strength for Flysch materials as well as to increased void ratio. Yalcin (2011) also stated that soils with a high content of fine particles are more likely to fail, thus clay-rich landslides are more likely to fail. Besides protection measures, spatial planning strategies as one example of avoiding hazard prone regions can be implemented to reduce damage (Crozier and Glade, 2005; Goetz et al., 2015). To develop effective approaches, spatially related research as well as local on-site knowledge on landslide internal structure, dynamics and triggering mechanisms is crucial (Marr et al., 2023; Shah et al., 2023).

Weak layers, commonly located between permeable and impermeable layers (Asriza et al., 2017), are thereby of particular importance for preconditioning landslide failures since they regularly function as slip surfaces (Soto et al., 2017; Rezaei et al., 2018). They often consist of saturated (silty) clays, mostly in a plastic state or close to their plasticity limit, which causes a high potential of failure due to their low shear strength (Soto et al., 2017, Rezaei et al., 2018). Materials with a high content of fine particles, such as clayey layers, can be expected to fail more easily (Yalcin, 2011) since the effective porosity of the soils is reduced by high clay content (Flores Orozco et al., 2022). Consequently, if they occur as spatially uniform layers characterized by low permeability, water logging can be often observed in the mass prone to landsliding (Yin et al., 2016; Soto et al., 2017; Rezaei et al., 2018). Hereby the pore pressure of these locations increases while matrix suction and effective stress decrease, until the shear strength declines to a critical value and a failure along the slip surface occurs, making it an important preconditioning factor for landslide triggering mechanisms (Schwenk, 1992; Friedel et al., 2006; Yalcin, 2011; Perrone et al., 2014; Asriza et al., 2017; Rezaei et al., 2018; Komolvilas et al., 2021). Those layers often act as slip surfaces for the overlaying mass (Schwenk, 1992; Komolvilas et al., 2021). Both Yin et al. (2016) and Rezaei et al. (2018) found that most of their investigated landslides showed weak permeable layers overlaying slip surfaces with a high clay fraction, low permeability and low shear strength. In particular after heavy precipitation, the saturation above the clayey slip surfaces often increased (Rezaei et al., 2018), which is indeed a result of their low permeability. Additionally, Soto et al. (2017) found that clay layers can act as a lubricant when they soften under increased saturation. Furthermore, Yin et al. (2016) determined that in addition to slip surfaces consisting of mostly clay particles, also the impermeable bedrock has the potential for act as a slip surface. Due to the lithological setting, both types of slip surfaces can be expected in the Flysch Zone (Figdor et al., 1990; Schwenk, 1992; Schnabel, 1999; NOEL GV, 2008) and therefore, their identification by applying different methods is the key goal of this study.

Electrical Resistivity Tomography (ERT) is widely applied to characterize internal landslide geometries and to locate features such as slip surfaces which determine to a great extend the mechanisms of failure. Thereby, it is often used in combination with direct methods such as borehole drilling and laboratory testing (e. g. Bell et al., 2006, Friedel et al., 2006, Merritt et al., 2014, Rezaei et al., 2018, Falae et al., 2019, Asriza et al., 2017, Stumvoll et al., 2020, Imani et al., 2021, Kaminski et al., 2021, Khan et al., 2021 and Komolvilas et al., 2021) or Dynamic Probing (DP) Tests (Friedel et al., 2006; Stumvoll et al., 2020; Komolvilas et al., 2021) for validation. Perrone et al. (2014) describe the results observed across different studies applying 2D, 3D and time-lapse ERT studies to understand spatial and temporal variations in landslides. Furthermore, some authors use multitemporal measurements or time-lapse ERT to monitor (seasonal) variabilities in the sub-surface, for example of flow paths or water content (Palis et al., 2017; Rezaei et al., 2018; Samodra et al., 2020). Whiteley et al. (2019) provide an overview of what geophysical methods are used in landslide research including different geoelectrical and seismic methods: Besides ERT also self-potential monitoring plays an important role in landslide investigation. Also, induced polarization (IP) or spectral induced polarization (SIP) as extension of ERT has also emerged as a suitable method for the investigation of clay-rich landslides (Flores Orozco et al., 2018; Flores Orozco et al., 2022; Gallistl et al., 2018; Revil et al., 2020). Complementary multitemporal UAV surveys (Samodra et al., 2020), airborne laser scanning (Kaminski et al., 2021), or GPS surveys (Merritt et al., 2014; Mantovani et al., 2022) are applied to detect surface movements in order to link sub-surface conditions to deformations visible at the surface.

At the Hofermühle landslide observatory, located in the Flysch Zone of Lower Austria, a variety of static and multi-temporal techniques are utilized since 2015 (Flores Orozco et al., 2022; Stumvoll et al., 2021; Stumvoll et al., 2022). Marr et al. (2023) have investigated spatial as well as temporal correlations of historical data records and long-term monitoring systems for slow-moving landslides in the Flysch Zone of Lower Austria, with the Hofermühle landslide as one of them. Their results show that landslides exhibited different characteristics despite similar conditions, and it was possible, to connect specific precipitation events to the measured landslide activity (Marr et al., 2023). Especially for non-linear behavior and variable displacement patterns, as we find at Hofermühle, learnings from historical data help to set up long-term monitoring systems appropriate to the site and are crucial to mitigate landslide hazards (Marr et al., 2023). The Hofermühle landslide is regarded as representative for other slopes in the Flysch Zone with similar meteorological and geological conditions, anthropogenic impacts and process dynamics. After definitions of Cruden and Varnes (1996), Dikau et al. (1996) and Hungr et al. (2013), the Hofermühle landslide can be described as retrogressive complex landslide with earth slide – earth flow like behavior. This landslide moves in phases of varying activity in different subsystems (Stumvoll et al., 2021; Stumvoll et al., 2022). According to Hungr et al. (2013) the displacement of earth flows is expected to occur during phases with slow movement along the main sliding surfaces, whereas internal shear is increased when a plastic mass forms that moves in a flow-like manner. Slow active landslides are mostly driven by changes in boundary conditions, especially rainfall events, or viscous deformations (Picarelli, 2007; Li et al., 2023). This characterization can be confirmed by the observations made so far at the Hofermühle landslide: whilst the main initial landslide activation was in 2011 and 2013, both (slow) rotational and translational sliding processes have been detected in recent years within the different subsystems. Respective extensions are connected to the main landslide, which again formerly depicted earth slide – earth flow like behavior. Both the combination of landslide types as well as their spatio-temporal interlinkages – very slow and very fast dynamics – define the complexity of the system (Stumvoll et al., 2021; Stumvoll et al., 2022). The analysis of ongoing surface and sub-surface dynamics is of great relevance to gain a better process understanding for this area (refer to noeslide.at for most recent information).

Based on this previous work, we focus on a combination of ERT as a non-invasive method to analyze sub-surface features, recognize patterns, and structures by gaining information on resistivity distributions in order to approximate the geometry of different layers in this study at the Hofermühle landslide. DP as a direct method is applied to validate the ERT data. While former studies by Stumvoll et al. (2022) already comprise sub-surface information of the Hofermühle landslide and data interpretation with respect to sub-surface structure, their focus has mainly been on the most recently active extensions of the main landslide (see Fig. 1b) and the currently more or less stable parts of the slope. The focus of this study lies on the sub-surface characterization of the main and initially activated landslide area. The specific objectives are

- to detect and characterize slip surfaces,
- to identify the total depth of the initially activated sliding mass, and

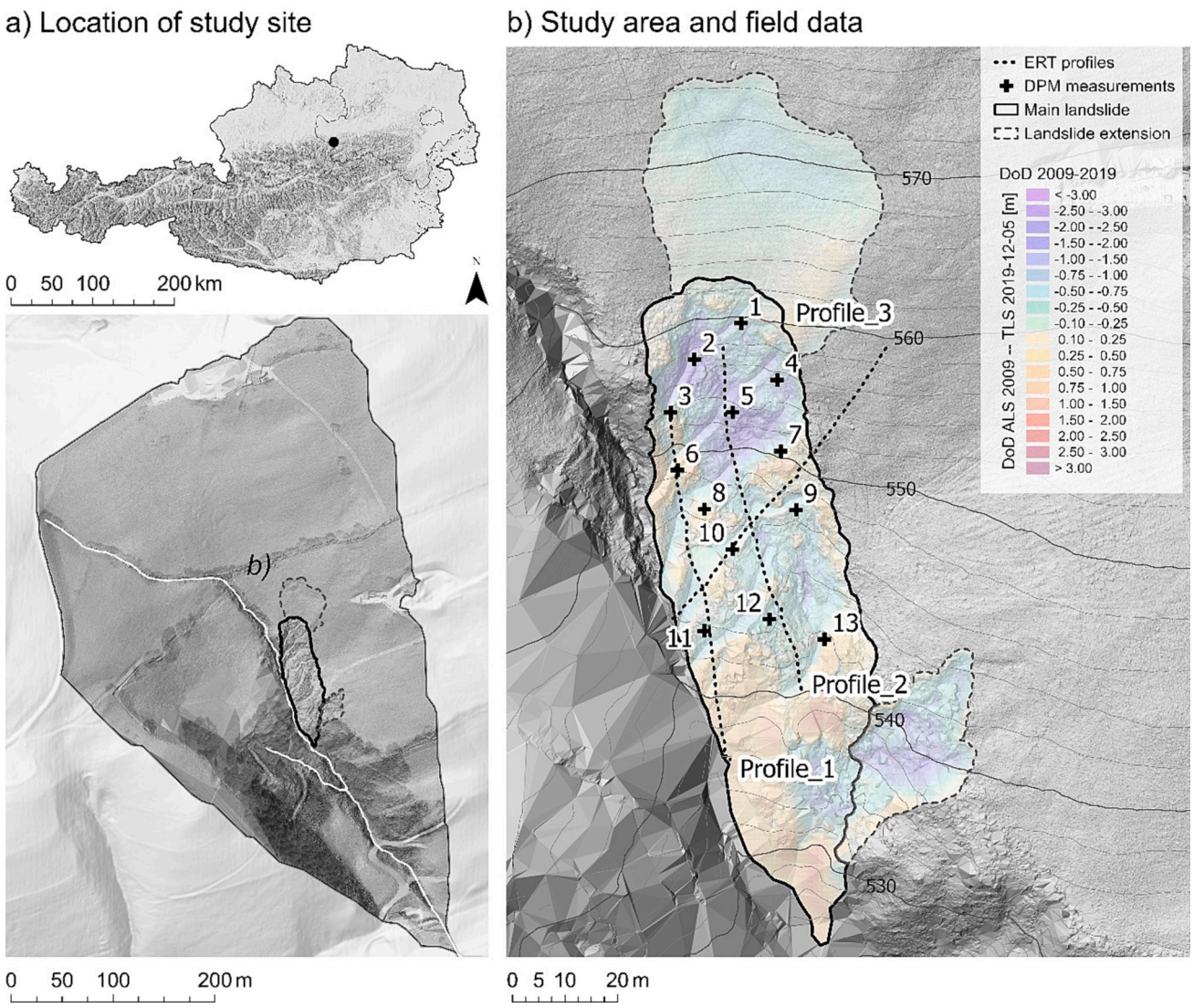

Fig. 1. a) Location of study area in Lower Austria, detailed view of the Hofermühle watershed, torrent is indicated in a white line. b) Overview on ERT profiles 1 to 3 and DPM measurements. Simplified morphological landslide features and changes in surface height between 2009 and 2019 are indicated by different colours. Relief shading in a) based on Austrian 10 m DEM (BMDW, 2015) and b) on a 0.05 m TLS-DEM (2019-12-05). DEM of Difference (DoD) calculation in b) based on 1 m ALS-DEM (NOEL GV, 2008) and 0.05 m TLS-DEM (2019-12-05). For details on mapping and DoD calculations refer to Stumvoll et al., 2021; Stumvoll et al., 2022).

- to differentiate single layers or bodies within the landslide mass as well as its geometry.

Since pore water pressure plays a major role in the initiation of landslides (Palis et al., 2017), this information is necessary in order

a) to estimate in which depths the landslide is likely to be re-activated,
b) to assess the potential volume of the displaceable mass under different scenarios and
c) to determine potential areas of water accumulation.

These conditions can be observed especially in clay-rich landslides (Schwenk, 1992; Friedel et al., 2006; Asriza et al., 2017; Komolvilas et al., 2021). Clay can form impermeable layers and then function as a hydraulic barrier, which can lead to accumulate water above these layers after prolonged or intense rain events, resulting in a higher pore water pressure and thus a higher probability of initiating landslide movement (Schwenk, 1992; Yalcin, 2011; Yin et al., 2016; Soto et al., 2017; Rezaei et al., 2018; Komolvilas et al., 2021). This mechanism has already been investigated in proximity to the study site, but not yet within the main and initially activated landslide area (Flores Orozco et al., 2022; Stumvoll et al., 2022). Consequently, this study focuses on this active landslide body.

2. Study area

The Hofermühle landslide, named after a local farm, is located near Konradsheim, Waidhofen a. d. Ybbs, district of Amstetten, Lower Austria (Fig. 1). Adjacent to the Northern Calcareous Alps, the area is situated within the geologically complex formation of the Flysch and Klippen Zone Flysch to the north (Figdor et al., 1990). The Flysch unit, at its broadest extension only ~10 km in width, contains thick regolith layers of weathered sandstone and clay-marl stones, which form loamy-clayey layers. As previous studies show, slip surfaces often form along the border of the weathered material and the basement rocks as well as above clay layers (Figdor et al., 1990; Schwenk, 1992; Schnabel, 1999; NOEL GV, 2008). Due to weathering, the clay content even increases making the formations more sensitive with respect to the influence of water content on slope stability (Anis et al., 2019).

The unit of the Gresten Klippen Zone was formed from deposits north of the Rheno-Danubian Flysch and south of the margins of the Bohemian Massif. As implied by the name, it forms several *Klippen* (German)

(Schnabel, 1999; Höck et al., 2005). At the study site, lime-sandstones, marl stones and clay are present. Within different sediment layers, *Konradsheim* limestone can be found. It contains matrix-supported conglomerates and sedimentary breccias, ranging up to hundreds of meters in thickness. The material underlies tectonic stress and is known to form a material called *Rutschtone*, which is especially prone to landslides (Figdor et al., 1990; Schwenk, 1992; Höck et al., 2005; NOEL GV, 2008). For more detailed information on local geology and lithology, please refer to Thenius (1974), Schnabel (1999), Schnabel (2002))and Höck et al. (2005).

Meteorological conditions support the weathering as well as the mobilization of slope materials. The mean yearly precipitation rate is 1196.03 mm with the highest values of 149.91 mm in July (mean 1896–2022). Long-lasting rainfall over two and more days as well as rainfall with >30 mm per day can be expected frequently (based on HISTALP data from Waidhofen a.d. Ybbs, period 1896–2022, refer to Auer et al. (2007) and Stumvoll et al. (2022) for more details). The monthly maximum in the period 1974–2019 at the nearby measuring station Hinterlug was 385 mm in August 2002, the maximum daily precipitation 130.50 mm on 6. September 2007 (for further information see eHYD WebGIS-application provided by BML, 2023: https://ehyd.gv.at/#).

The catchment area of the Hofermühle-torrent with a length of 0.64 km and an area of 0.17 km^2 extends from an altitude of 620 m a.s.l. in the highest part to 460 m a.s.l. at the mouth into the preflooder Redtenbach, which drains the Redtenbach valley with an altitude difference of 655 m. The main landslide area covers an elevation range of about 520 m - 560 m a.s.l. and while the hillslope in the upper part of the Hofermühle landslide is relatively shallow at 5° - 20°, it is predominantly 15° - 30° in the lower third; in some areas even up to 45° (Stumvoll et al., 2021). With a length of 9.05 km and an area of 15.55 km^2 the Redtenbach forms a sub-catchment of the Waidhofenbach. The catchment area of the Hofermühle torrent can be seen as representative for other tributaries in the Redtenbach valley as well as in the rest of the Flysch Zone in terms of climatic and geological predisposition as well as anthropogenic landuse and related impacts on hillslope hydrology (see also Stumvoll et al., 2021). The combination of steep slopes and high clay content, leads to reduced slope stability, causing the Flysch and Klippen Zone therefore to being exceptionally prone to landslide processes. This has been investigated intensively by inter alia Figdor et al. (1990), Schwenk (1992), Terhorst and Damm (2009), Bell et al. (2011), Petschko et al. (2013, 2014), Anis et al. (2019), Stumvoll et al., 2020, Stumvoll et al., 2021, Stumvoll et al., 2022) and Steger et al. (2022). It is known for many decades, that heavy rainfall, high rates of snowmelt and anthropogenic interference are the main triggers of landslides in this region (Schwenk, 1992). The distribution of registered landslides in the broader area clearly states a link with the present lithology (e.g., Schwenk, 1992; Bell et al., 2011). Respective records prove, that most landslides are located in the Flysch Zone and Klippen Zone – especially in the western part of Lower Austria. Landslide susceptibility maps reinforce this correlation: the highest landslide susceptibilities are presently in the Flysch Zone (Petschko et al., 2014; Goetz et al., 2015; Lima et al., 2017).

The Hofermühle landslide is closely connected to the eponymous torrent. For detailed and most recent information on the study sites landslide history, possible triggering mechanisms and monitoring setups refer to Stumvoll et al. (2021), Stumvoll et al. (2022) and Flores Orozco et al. (2022). Even though former landslide movements can be assumed, first displacements were documented in the late 1970's (Sausgruber, 2013) to the orographic right of the torrent (see Fig. 1a). In 2011, displacements defined as rotational sliding were registered to the orographic left in a forested area. A subsidence of 2 m occurred within two weeks (Kotzmaier, 2013; Sausgruber, 2013). The same area was reactivated in 2013. A waterlogged section forming the lower part of the displaced mass developed into a debris flow with velocities up to 20 m/h (Sausgruber, 2013; Sausgruber, 2016) (see also Fig. 1b, area defined as main landslide and respective changes in surface height). Two extensions of the main landslide area were activated during this event (Fig. 1b, landslide extension, see also Stumvoll et al., 2021). As an immediate mitigation measure, and finalized in 2018/2019, a dam has been built by the Austrian Service for Torrent and Avalanche Control (*Wildbach und Lawinenverbauung* (WLV)) near the outlet of the catchment to protect the resident houses located in the area of debris deposition (Sausgruber, 2013, Sausgruber, 2016). The landslide surface was altered by deforestation and the new surficial drainage channels in the main landslide area, build by the WLV in 2019 to divert surficial run-off directly into the Hofermühle torrent by the WLV in 2019 (see trenches in DEM in Fig. 1b). During fieldwork in 2020, these trenches were waterlogged again. Changes in surface morphology, landslide features, and surface height indicate ongoing movement (Stumvoll et al., 2021). The agriculturally used pasture above and close to the landslide area is heavily influenced by additional drainage pipes (see Stumvoll et al., 2022). The location of the drainage pipes is well known for the most recent installation; however, the position of pipes installed many decades ago is rather vague. The influence of broken drainages with respect to punctual entrainment – and subsequently landslide preconditioning and possibly even triggering – cannot be neglected for the parts adjacent to the main landslide body.

Due to its long-lasting spatiotemporal activity, the Hofermühle landslide is intensively investigated and monitored with a variety of direct and indirect surface and sub-surface investigations (for detailed information refer to Stumvoll et al., 2021, Stumvoll et al., 2022, Flores Orozco et al., 2022). Since 2015, the site is part of the long-term landslide observatory in Lower Austria (University of Vienna - NoeSLIDE, 2022 – refer to https://www.noeslide.at/index.php/de/hofermuehle for details) and the respective site is additionally embedded in the LTER-Austria (Long-term Ecological Research - https://www.lter-austria.at/). Previous studies show that surface investigations indicate complex landslide behavior, regarding both temporal occurrence (main activity 2009–2015, afterwards decreasing but ongoing) and changes in landslide processes (initial sliding developing into flowing - Stumvoll et al. (2021). Sub-surface monitoring data (Stumvoll et al., 2022) as well as a comparative approach using induced polarization (IP) measurements (Flores Orozco et al., 2022) give first insights into sub-surface structure, groundwater level and flow patterns, regolith thickness and areas, and respectively layers of potential groundwater accumulation and landslide activation. However, these studies focus on the newly activated landslide extension(s) as well as the surrounding slope to the east, which might be affected by landslide activity in the future (see also Fig. 1b). Only little is known about the main landslide area and its subsurface conditions apart from first descriptive geotechnical reports by the WLV (Sausgruber, 2013, Sausgruber, 2016) and changes in surface height computed with multi-temporal DEM comparison (Stumvoll et al., 2021, Stumvoll et al., 2022). Hence, the main objective of this study is to also explore the sub-surface conditions in this landslide part applying direct and indirect methods. This area is currently understood as a source for future debris flow activity in the lower part and landslide movement in the upper areas due to toe unloading.

3. Methods

This research is based on a combination of three ERT profiles and 13 DPM measurements (see Fig. 1b). ERT is applied as a non-invasive, cost-effective method providing information about sub-surface variations of the electrical resistivity on a large scale, with the DPM used to gain ground truth as validation at specific locations. The DPM measurements were performed on 12.03.2020 to get an overview about bedrock geometry, regolith cover and landslide mass. Implications from these measurements regarding the required accuracy and depths of special interest were used to determine the location and configuration of the ERT profiles measured on 14.05.2020.

3.1. Electrical resistivity tomography (ERT)

The interpretation of ERT data provides indirect information about variations in the electrical resistivity the sub-surface, which is dependent on the water saturation, fluid conductivity, porosity, and surface conductivity. In particular, surface conductivity dominates as the main conduction mechanism in presence of materials with high surface area and surface charge such as clays and organic matter (e.g., Flores Orozco et al., 2022). Hence, interpretation of ERT results permits to e.g., identify lithological and mineralogical changes, soil composition, and, in combination with direct methods, permeability can be derived (Merritt et al., 2014; Perrone et al., 2014; Asriza et al., 2017; Rezaei et al., 2018). In landslide investigation, ERT is especially adequate for the exploration of stratigraphic features and their spatial extent, fracture zones (Perrone et al., 2014; Scapozza and Laigre, 2014; Asriza et al., 2017; Rezaei et al., 2018) and areas of water accumulation and preferential flow paths, which are related to the build-up of pore-fluid pressure (Palis et al., 2017). This factor usually plays a key role in the initialization process of landslides (Palis et al., 2017) and can consequently be used to forecast points of local failures (Flores Orozco et al., 2018). As a non-invasive method, it does not disturb the landslide mass during the data collection (Wenner Wenner, 1915, Imani et al., 2021), which is especially important on unstable slopes and can be used to reduce the number of drilling points used within geotechnical methods (Falae et al., 2019; Imani et al., 2021). These geotechnical methods are more time-consuming and expensive and only provide point data along a given depth profile (Rezaei et al., 2018).

The focus thereby is to determine in this central body the boundary between a permeable and an impermeable layer, which can be assumed to be the depth of future slip surface(s) (Asriza et al., 2017). Considering the lithology of our study area, studies have shown that it is likely that slip surfaces occur in clayey material, in addition to those located directly on the bedrock (Figdor et al., 1990; Schwenk, 1992; Schnabel, 1999; NOEL GV, 2008). Furthermore, we want to get additional information of areas of water accumulation and heterogeneities of the subsurface structure and materials by applying geophysical methods such as ERT. When interpreting measured resistivity values, it is important to note that although clayey soils are, due to the contribution of surface conduction in presence of materials with high surface area and surface charge such as clays and organic matter, associated with the lowest resistivity values, estimating the hydrogeologic properties of the subsurface can still be challenging because of the need to distinguish between the contribution of clay content and that of a high water content (Flores Orozco et al., 2018). Previous studies show, however, that respective ERT values fall in a wide range for expected alike conditions (Bell et al., 2006; Sass et al., 2008; González-Álvarez et al., 2016). Especially for clay-rich materials, surface conduction along the electric double layer formed at the solid-liquid interfaces can play a dominant role wherefore it can be difficult to distinguish what causes high conductivities (Flores Orozco et al., 2018). Nevertheless, we assume that water accumulates above impermeable layers, and we further conclude, that these layers are composed of clayey material. Therefore, it is expected that high conductivity will occur due to both the surface conduction of the clays and a high water content (Rezaei et al., 2018), and thus, this area in the sub-surface can be detected with ERT.

The resolution In ERT data ranges from millimeters to kilometers depending on the spacing and configuration of the electrodes (Akingboye and Ogunyele, 2019). The method is based on the injection of an electrical current (I) across an electrode dipole (figuring as a transmitter) and the measurements of the resulting potential difference (V) in another pair of electrodes, with tens to hundreds of electrodes used to resolve vertical and lateral variations in the electrical resistivity (Binley and Kemna, 2005).

In this study, ERT data were collected with a Syscal Pro manufactured by Iris Instruments along three long profiles with 1 m electrode spacing, with two short profiles of 35 m length with higher resolution of 0.5 m spacing between the electrodes co-located within the long profiles as depicted in Fig. 1b. The different electrode spacing was to reach deeper areas of investigation (favored by the large electrode spacing) and gaining information with high resolution (favored by the small electrode spacing) in the selected area. We used a dipole-dipole measuring scheme with all levels and dipole lengths of 1, 4 and 6 times the electrode spacing (skip 0, 3 and 5 configurations). All measurements were collected as normal and reciprocal pairs, with reciprocals referring to the repetition of the same quadrupole after changing the electrodes used for current and potential dipoles. Analysis of the misfit between normal and reciprocal readings was used to identify outliers and quantification of data error (see Flores Orozco et al., 2012; Flores Orozco et al., 2018). Erroneous measurements associated to negative apparent resistivity values or current injections were also filtered prior to the inversion, for this step, the geometric factor of each quadrupole was modeled to take the topography changes into account. The inversion of the data was conducted with CRTomo (by Kemna, 2000), which allows the inversion of the data to a confidence level given by an error-model. Normal-reciprocal analysis resolved for an absolute error of one mΩ and a relative error of 5 %. In the inversion results, we blank out model parameters related to low sensitivity values (< -2, computed from the logarithmic normalized values of the cumulated sensitivity). Previous studies have revealed the possibility to use the sensitivity as a proxy to evaluate the uncertainty of the inverted results (e.g., Flores Orozco et al., 2013; Weigand et al., 2017).

3.2. Dynamic probing Medium (DPM)

Dynamic probing was conducted with a medium-weight hammer of 30 kg and a drop height of 0.50 m in 13 different locations, counting the number of blows to push the rod with a 43.7 cm diameter cone 10 cm into the ground. The resulting values can be used, to estimate the penetration resistance, relative density and friction angle of the subsurface in different depths. Based on the required energy to push the cone in the ground, the soil strength, which is crucial to understand the trigger mechanisms of complex landslides, can be estimated (Avanzi et al., 2013a,Avanzi et al., 2013b, Komolvilas et al., 2021). In our study, derivations from the gained information are compared relatively and used to detect heterogeneities – e.g., separation planes – and approximate the depth of the sliding mass in different locations.

DPM measurements provide point data along a vertical profile, which alone are not sufficient to represent complex settings. Furthermore, the influence of grain shape, grain size and its distribution, roughness, groundwater and cone parameters are neglected. It is not possible to differentiate between point resistance and surface friction. When comparing data of this study site with data from other areas gained by other personnel, empirical correlations have to be treated with great care as a consequence of different equipment and lack of comprehensive standardization (Avanzi et al., 2013a, Avanzi et al., 2013b, Liebetruth, 2014, ÖNORM EN ISO 22476-2). Nevertheless, an integrated approach of DPM and ERT allows complementary information and therefore reduces the limitations of each method (Falae et al., 2019).

4. Results and discussion

In order to assess the overall sub-surface pattern of the active landslide mass, different profiles have been sampled. Profile 1 and 2 are located parallel to the torrent, with profile 1 being the closest to the natural drainage line (white line in Fig. 1). These profiles are located in the area where drainage channels on the surface were implemented (visible in Fig. 2). Profile 3 runs lateral to the other two profiles.

4.1. DPM

All DPM measurements (see Fig. 3 for a representative selection of

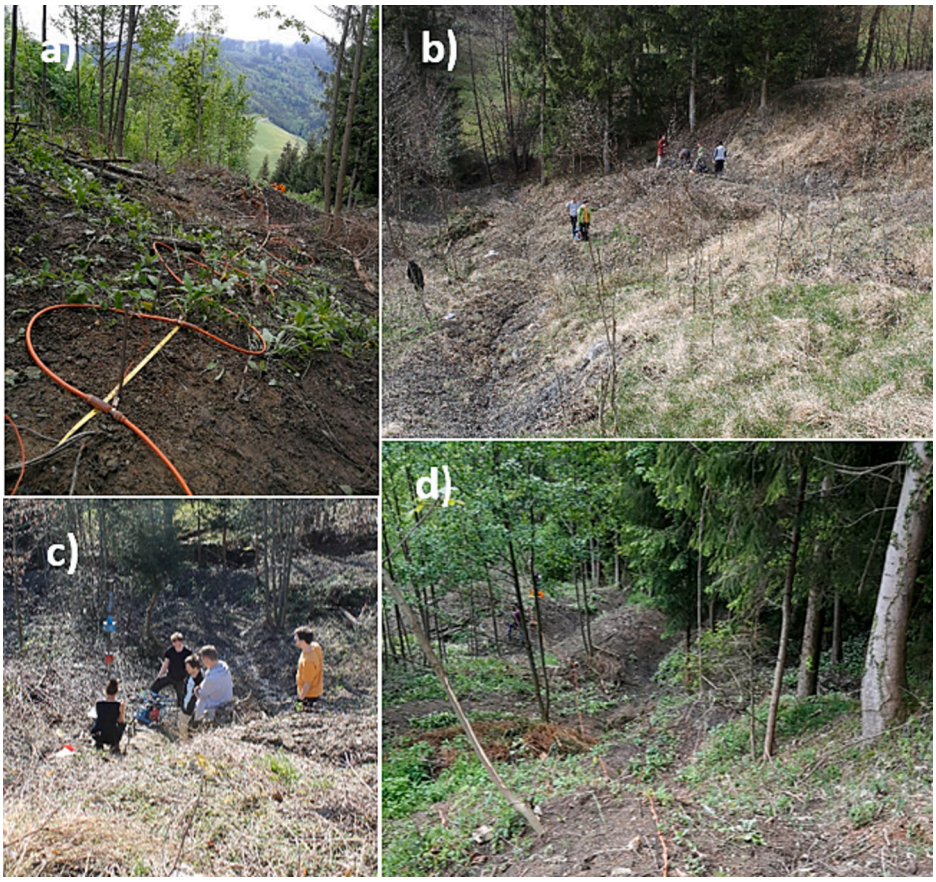

Fig. 2. Fieldwork on the Hofermühle landslide. a) and d): ERT measurements conducted on 14.05.2020 (J. Luhn). b) and c): DPM measurements conducted on 12.03.2020 (M. J. Stumvoll-Schmaltz). Surficial drainage channels are visible in all pictures.

DPM plots) display very loose - loose material close to the surface in variating thicknesses 0.6 m to 1.9 m, which is composed of the disturbed landslide mass. In this area, we can expect a favored infiltration for water since infiltration depends on the compaction as well as the porosity and void ratio of the soil materials (Yalcin, 2011). Below these depths, we find in some DPM measurements a relatively uniform increase of the penetration resistance in the weathered material up to the potential bedrock (DPM 2, 12). In some cases, the (very) loose disturbed landslide mass even reaches down to the potential bedrock (e.g., DPM 1, 11), while we find more firmly bedded layers above the bedrock in other locations (e.g., DPM 4, 6, 9). All those can be interpreted as areas of intense weathering of the bedrocks and consequently a reduced strength. In contrast, the other DPM measurements show interbedded layers of higher penetration resistance (DPM 3, 5, 7, 8, 10, 13). These layers might consist of slope debris material from the Holocene periglacial period, where surface displacement by solifluction on the former permafrost occurred (for information on alpine solifluction in the Holocene see Jaesche et al., 2002, Veit, 2002 and references within). Within past solifluction in steeper terrain, surface material might be incorporated into deeper layers during former movement. In the case of DPM 8 at 2.1 m, the higher penetration resistance might indicate the presence of a stone that locally increased the number of blows. In addition to changes in the compaction of the sub-surface material, the presence of slip surfaces, individual residues or changes in saturation can also be the cause of variable strengths of the sub-surface materials.

4.2. ERT

Fig. 4 shows the resistivity imaging results including the position and depth of the overlapping DPMs, as well as the indication of the depth and shape of the potential slip surface.

4.2.1. Profile 1

In the first 12 m of profile length, a change from medium resistivity values just below the surface (about 100 Ohm.m) to lower values (about 30 Ohm.m) starting at about 2 m depth at the potential position of the bedrock can be observed. Between 17 and 52 m profile length the higher resolution data from profile 1 has been measured with 0.5 m electrode spacing. The surface drainage channels build by the WLV intervention in 2019 are clearly visible in the surface shape of the profile. Due to the accumulation of water on the surface, which was observed during the measurements in the form of the formation of puddles in the trenches, we can conclude that a high clay content as well as compaction due to the construction works during the installation of the trenches, hinder the infiltration of water at the surface. This is reflected by low resistivity values in those areas (below 10 Ohm.m) and the surrounding subsurface in 23–33 m profile length. In approximately 3–5 m depth in 20–38 m profile distance a shift in resistivity to approximately 40 Ohm. m is visible, which can be interpreted as a potential slip surface on the bedrock increasing in depth from about 2 m at the beginning of the ERT section until about 5 m depth at 35 m profile length. From the resistivity values and observations during the measurements, we can assume that the subsurface materials near the drainage channels are saturated, but dryer upslope, where drainage channels are not present and higher resistivity values in the loose sub-surface are found. In addition, it can be assumed that clay particles are transported during rainfall events with surface runoff into the drainage trenches, resulting ultimately over a longer period in higher clay content here.

The higher resolution 0.5 m spacing in profile 1 shows a high variability of the measured values just below the surface. This might be the

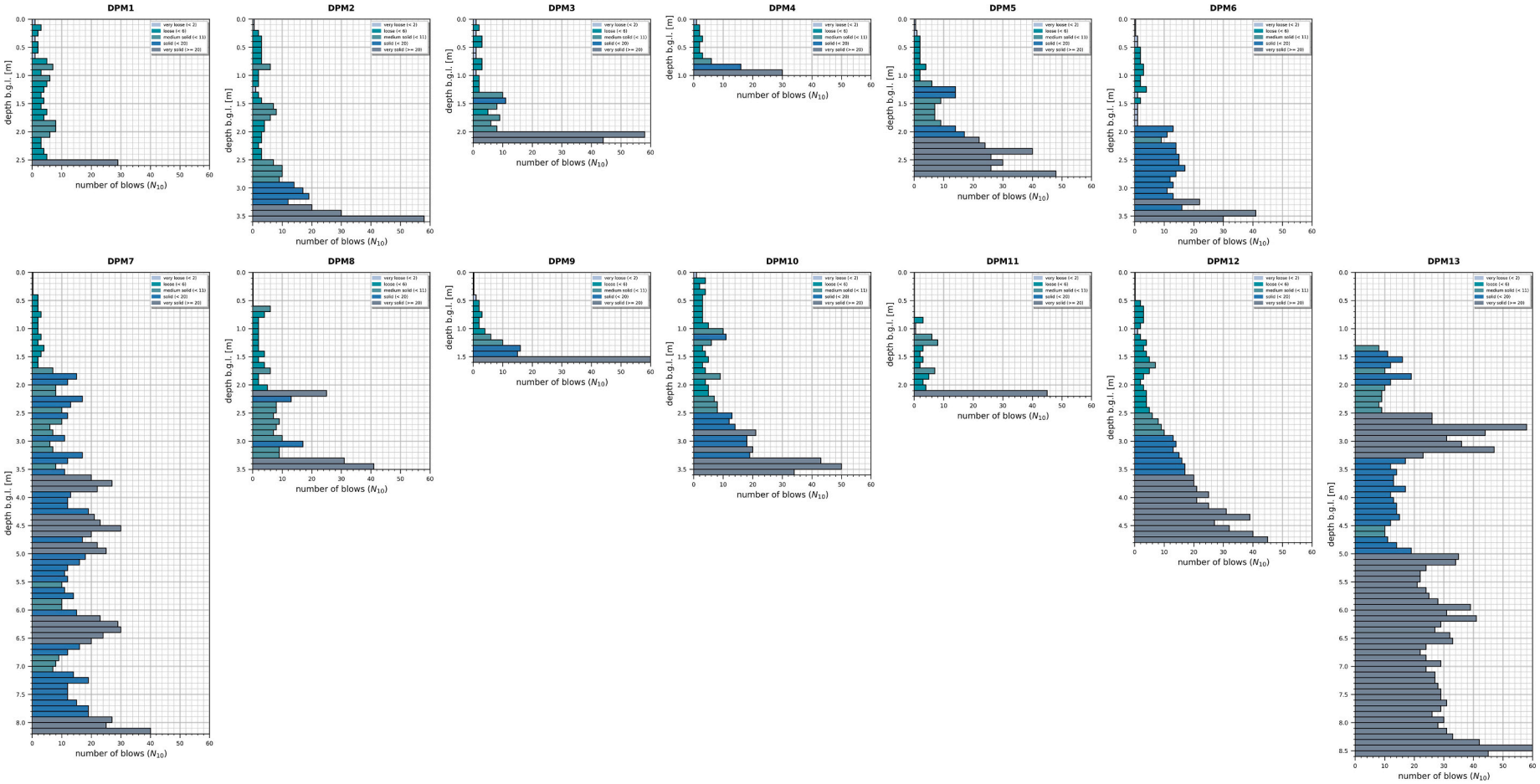

Fig. 3. Selection of the DPM measurements conducted on 12.03.2020. The required number of blows per 10 cm depth was divided in categories of penetration resistance ranging from very loose – very solid material. Refer to Fig. 1 for location on the landslide.

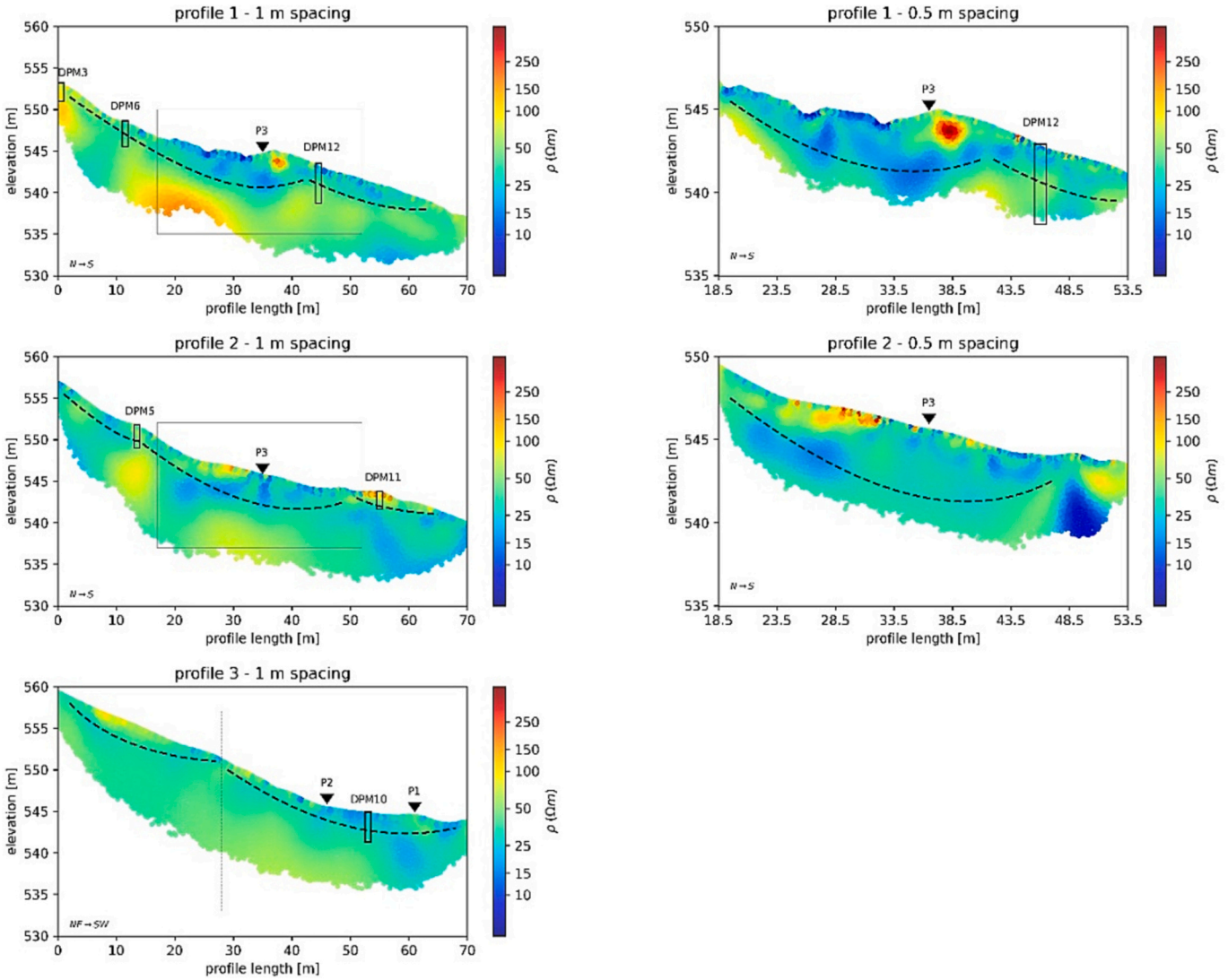

Fig. 4. ERT images of the resistivity distribution in profile 1, profile 2, and profile 3 – on the left side with 1 m spacing, on the right with 0.5 m spacing for the respective profile. Overlapping or nearby located DPMs are indicated. The dashed lines indicate the position of the interpreted slip surfaces. The dotted line in Profile 3 shows the distinction to the initially activated area. Triangles mark where the profiles overlap.

result of the surface alterations, where material was relocated and compacted leading to water logging in the trenches. Furthermore, between 34 and 42 m profile length the low resistivity is superimposed by material with the highest resistivity (up to 300 Ohm.m), which most likely consists of excavated material that was piled up during the excavation of the drainage trenches right next to them.

Between 40 and 60 m profile distance the ERT measurement shows low resistivity values (predominantly below 30 Ohm.m) until 1–2 m depth, below which the values rise to about 50 Ohm.m which we interpret as the presence of deeply weathered bedrock material. Changes of textural parameters of the bedrock are expressed in varying resistivity values covering a relatively wide range from about 20 Ohm.m up to 150 Ohm.m. Between 0 and 5 m and 12–30 m profile length, resistivity values are higher than 100 Ohm.m, whereas the other materials interpreted as bedrock range mostly between 25 and 70 Ohm.m. This is likely a result of different textural properties of the bedrocks since the Flysch Zone is characterized by heterogeneous compositions of predominantly clays, marls, sandstones and siltstones (Figdor et al., 1990; Schwenk, 1992; Schnabel, 1999; NOEL GV, 2008; Anis et al., 2019).

4.2.2. *Profile 2*

As in profile 1, higher resistivity values (mostly between 50 and 100 Ohm.m) occur in the first meters of the profile, with the very solid material being reached at about 2 m depth, making this section relatively shallow. In contrast, between about 25–50 m profile length, as already recognized in profile 1, a comparatively deep body of about 3–5 m depth is found, which shows lower resistivity values (about 15–30 Ohm.m). Beneath, resistivities around 50–100 Ohm.m indicate that the bedrock is reached. Between about 20–30 m profile length, this body is superimposed by a layer with higher resistivities (mainly around 100 Ohm.m) in the first 1–2 m directly below the surface.

In profile 2 0.5 m spacing has been applied resulting in a higher resolution supplementary data between 17 and 52 m profile length. Here we find a high variability of resolved resistivity values directly below the surface as we could also find in profile 1 0.5 m spacing. The area with resistivity around 10 Ohm.m between 30 and 35 m and 2.5–10 m depth in profile 2 0.5 m spacing correspond to the low values observed also in the imaging results obtained with the measurements using 1 m electrode spacing. From 52 to 62 m profile length, we see relatively high resistivities up to 200 Ohm.m in the first 1–2 m below the surface, below which the values drop to about 25 Ohm.m in the underlying material we interpret as bedrock. The feature in the image with the smaller electrode spacing has a larger extension into depth than in the image resolved with larger electrode spacing. This inconsistency is an artifact resulting from

the loss of sensitivity at depth at both ends of the ERT profiles. The lack of deep measurements at the ends of the profile hinders the ability of the method to detect the end of high conductive anomalies close to the surface. The high clay content near the surface results in high current densities near the electrode, which limits the information obtained at depth.

4.2.3. Profile 3

Profile 3 runs towards the torrent and perpendicular to the two other profiles, crossing them in their middle length. In the upper part, between 0 and 28 m, we can identify 2 layers above the potential bedrock, which shows resistivity values about 50 Ohm.m. The subsurface material with resistivity values about 30 Ohm.m is superposed by a layer with resistivities about 100 Ohm.m between 3 and 19 m. Stumvoll et al. (2021) also showed that the more recently activated landslide extension located north of the main landslide (see Fig. 1), which has characteristics of a rotational landslide, forms an accumulation area located just above profile 3 (see Fig. 1: DoD 2009–2019). As already implied by Stumvoll et al. (2021), an interrelation of the landslide extensions with the main landslide is likely at different spatio-temporal scales. Therefore, the upper layer could consist of compacted material that is being pushed down by the rotational sliding activities taking place directly upslope.

At 28 m profile length the break-off edge of the last event is located (indicated with a fine dashed line in Fig. 2). A transition between two active layers with different slip surfaces can be found here. Since previous movements already displaced material in 2013 (Sausgruber, 2013), the section below 28 m displays the shallower remains of material above the bedrock after the former event. In Fig. 1, this transition is visible as well from the DEM. During the event masses above an upper slip surface has been displaced. Consequently, one possible interpretation is that the upper slip surface, which we approximate from 0 to 28 m, extended to the torrent above the current landslide body in this area before it was activated and caused the mud flow. In other parts of the Hofermühle-landslide outside this most active area, investigations have also indicated separated slip surfaces at different depths (see Stumvoll et al., 2022). Based on those findings, it is assumed that the current slip surface after the transition is now located on the bedrock.

In general, the section from 0 to 40 m shows higher resistivity values on the bottom of this layer compared to the section from 40 to 70 m. This might indicate the relocation of clay minerals downslope with the surface runoff, as we find low resistivity values especially in the vicinity of the drainage channels that act as preferential flow paths and additionally it gives an idea of the thickness of the active layer above the slip surface.

4.3. Interpretation of the merged results

4.3.1. Profile 1

DPM 3 is located close before the first electrode of profile 1 (see Fig. 1): It contains mostly very loose – loose material until a depth of 2 m, where the compacted materials we interpret as bedrock were found. In the ERT image, the transition to bedrock is associated with higher resistivity values (up to 150 Ohm.m) at this location. Such contrasts between loose and compacted materials were found on site before (Flores Orozco et al., 2022) and in other clay-rich landslides (Flores Orozco et al., 2018). DPM 6 is located at 11 m profile length. It shows very loose - loose material until 1.9 m depth below where the material is mostly solid, which we interpret as weathered material, to a depth of 3.2 m where the DPM indicates the presence of the very solid material interpreted as less weathered bedrock (please note that the terms ‘solid’ and ‘very solid’ do not refer to characteristics of the interpreted bedrock, but to the categories of penetration resistance, see Fig. 3). The resistivity image shows only minor changes here.

DPM 12 is located at 44 m profile length and reached a depth of 4.8 m with a relatively constant increase of penetration resistance with depth, reflected by a rise in resistivity from approximately 15–25 Ohm.m in the very loose – loose material (number of blows <6) to 70–100 Ohm.m in the material with higher penetration resistance (number of blows >11). The layer with highest penetration resistance was reached approximately 1 m deeper than in DPM 6 and 2 m deeper than in DPM3, indicating that more landslide material is accumulated above the bedrock in downslope direction. Additionally, DPM 8 and DPM 10, which are located at close distance and on the height of the presumed sliding mass between profile 1 and 2, provide similar results. The ERT measurement also indicate the position of the bedrock by an increase of resistivities and the loose material with lower resistivities not deeper than 3 m until 60 m profile length.

It can be concluded that the disturbed landslide mass above the bedrock in this area is loose and thus, water can easily infiltrate from the surface up to the bedrock, where the more solid material reduces or possibly even prevents infiltration. In addition, it can be assumed that weathering is higher in the disturbed mass, leading ultimately to an increase of clay content (Anis et al., 2019). This might explain the reduced resistivity at the potential bedrock surface beneath the landslide mass. A clay-rich layer below the loose material increases the sensitivity to failure due to water infiltration (Anis et al., 2019) as well as the more solid material forming the bedrock or deeply weathered bedrock. Combining all the information, it can be assumed that between 20 and 35 m profile length above the bedrock, clay-rich, loose and highly saturated material that is particularly susceptible to further movement and might act as a sliding surface, can be found. In addition, the thickness of the soil material located on the bedrock and additionally the saturation increases downslope to this area, suggesting that displaced material accumulates in this area.

4.3.2. Profile 2

DPM 5 is located at 13 m profile length. Until 1.1 m depth, the subsurface contains very loose – loose material. In 1.2 m depth, a 20 cm strong layer with high penetration resistance (required number of blows = 14) is embedded between medium solid material. At 2.1 m depth, the material with highest penetration resistance we interpret as bedrock was reached. The ERT shows values around 70 Ohm.m at this position, which can be explained by the surface alterations: The DPM 5 was conducted on piled up excavation materials whereby a drainage channel is located at about 7 m resulting in lower resistivities for the surrounding area (see Fig. 1). Still, the ERT image shows a larger structure below the depth reached by DPM that can be interpreted as bedrock. For the part from 0 to 13 m profile length, we can assume a similar depth of landslide material above the bedrock.

Between 17 and 52 m we can draw the same conclusions as already in profile 1: a thicker body of loose, clay-rich and saturated material above the bedrock at 4–5 m depth. The thickness of the loose reworked landslide mass can also be confirmed by DPM 8 and DPM 10, which were conducted between the profiles 1 and 2: Here, the potential bedrock is reached at about 3.3 m depth, which is deeper than at DPM 5 and DPM 11 at the beginning and end of the section of profile 2. It can be concluded that the movement-prone mass, which is also visible in the middle part of profile 1, extends into the section of profile 2 with a higher saturation and clay content in the area of the surface drainage channels, which are the preferred runoff paths (see Stumvoll et al., 2022), but which act as well as lines with higher infiltration and subsequent percolation of soil water leading to an increase of moisture in these subsurface areas.

DPM 11 was performed between two drainage channels on the piled-up excavation material at 54.5 m profile length reflected by resistivities up to 150 Ohm.m. The soil material is very loose until 0.8 m depth, which was reached with one blow of the DPM. Below, the material is mostly loose with a few medium solid layers (number of blows 6–10) until the very solid material in 2.1 m depth, displayed by a decrease in resistivity to 25 Ohm.m. Thus, this material seems to be very loose and highly saturated.

4.3.3. Profile 3

The DPMs located close to the transition from the surrounding regions of the Hofermühle landslide to the initially activated main landslide area, which is the focus of this study (indicated by the vertical dashed line in Fig. 3). This change is after 28 m profile length. Additionally, the DPM's 7, 9 and 13 show significant changes. Both DPM 7 and 13 were the deepest measurements, where several very solid layers between more loose material were present. These can be interpreted as slope debris blankets from the periglacial period (for information on alpine solifluction in the Holocene see Jaesche et al., 2002, Veit, 2002 and references within). However, it might also be that more solid rock fragments were hit, possibly also related to former slope debris. In contrast DPM 9 was very shallow, which corresponds to the interpretation from the ERT image indicating a very shallow landslide mass in this area.

One possible explanation for the high variability of landslide depths at the transition line is that the bedrock has different depths and deeper areas, possibly former bedrock depressions formed in Holocene periods, are now filled by former periglacial materials, which is now reworked landslide material. This might result in the observed depths of DPM 7 and 13. Variations in the composition of the bedrocks must also be considered, as well as a varying weathering intensity which might have reduced the material strength. Another theory is that the displaced masses of the contiguous complex landslide east of the active area are pushed downslope towards the torrent with a time lag and different phases of activity, resulting in different bulges. Different phases of activity are already known at Hofermühle (Stumvoll et al., 2022). Furthermore, the material has already been displaced by previous events, which could also be a reason for the different depths of the landslide body. Stumvoll et al., 2022 found that the thickness of the regolith is lower in areas associated to recent as well as former activity, whereas the regolith can form layers of up to 13 m thickness in more stable areas. This is consistent with our data at the transition zone. Furthermore, the comparison of the DPMs located at the upslope border to the active area (DPM 1, 2, 3 and 4) are shallower, which indicates as well that material is moving downslope away from the outlines of the active area.

4.4. Implications for the active area

Merging all information, movement within the slope and a mobilization of masses in the downslope direction of a vector between the southward direction and towards the torrent as well as a resulting accumulation in the area closer to the torrent can be assumed. All profiles show a body consisting of disturbed landslide materials potentially highly susceptible for mobilization due to a low penetration resistance and partly an assumed higher water saturation over the less permeable firm weathered material and even more solid, less weathered material we interpret as bedrock. This matches with the results from Stumvoll et al. (2021), Stumvoll et al. (2022), who found that slow sliding processes in the upper part of the Hofermühle-landslide slowly distribute material towards the Hofermühle-torrent to the currently very active part, which function as initiation locations for faster flow processes – as has been investigated in the past (Kotzmaier, 2013; Sausgruber, 2013). This process of material shift and the interaction of the main landslide area with the landslide extensions can also be traced by surface forms and their development in the period 2009–2019, which were described in detail in Stumvoll et al. (2021). They include changes in slope curvature; scarps, steps and banks; single forms as depressions and bulges; areas of stepped or undulating relief and process areas. In particular, scarps can be considered in direct relation to landslide activity. They occur in extensions adjacent to the main landslide area and show a connection to the differences in elevation (DoD) shown in Fig. 1. In Stumvoll et al. (2021) the numerous scarps before the 2013 event are recorded, as well as after the event and the implementation of the drainage channels where distinct surface changes (e.g. an enlargement of the landslide extension areas and the formation of main and minor scarps, respectively the formation of a new head scarp or retreat of the main scarp in upslope direction) in the area of the landslide extensions can be recognized. For more details see Stumvoll et al. (2021).

The DPMs support the interpretation of ERT results and deliver matching results regarding the depth of landslide mass and bedrock surface, which are considered as the potential slip surfaces. Based on the investigations, more precise sub-surface geometries can be assumed. Stumvoll et al. (2020) found that the information gained by dynamic probing tests was sufficient to detect slip surfaces for another landslide in the Flysch Zone, as well, which supports our investigations.

Another implication from our data is that clay particles are eroded by surface runoff and transported through, and partly deposited in the areas surrounding the drainage channels, leading to lower resistivity values in those areas due to a higher clay content as well as a higher saturation compared to the regions outside the highly active landslide in the upper parts. This theory is reinforced by surface run-off flow paths calculated by Stumvoll et al. (2022), which are mainly in the drainage channels towards the torrent. Before these drainage channels have been build in 2019, the run-off flow paths joined the torrent further downslope after crossing the study area (Stumvoll et al., 2022). Flores Orozco et al. (2022) interpreted that the northern as well as the southern part of the landslide system shows a higher clay content than the middle part. This supports the theory of fine particles as clay being eroded and accumulated further downslope at the surface and have then been integrated into the landslide mass during movement. Due to the constant movement of the active landslide part, all investigations on the site show indeed high variabilities in the sub-surface regarding clay and potential soil moisture as well as the depth of the bedrock (Stumvoll et al., 2020; Stumvoll et al., 2022; Flores Orozco et al., 2022). This is especially visible at the transition to the eastern part of the Hofermühle-landslide where the thickness of regolith varies the most.

We also find layers of decreased resistivities directly above the interpreted bedrock, which are probably a consequence of an increased clay content due to weathering (Anis et al., 2019) and to remolding of materials during creep. Since high saturation leads to a decrease in soil cohesion and shear strength as well as an increase in pore pressure (Anis et al., 2019), we can expect predisposing factors which can lead to sudden activation after intense or prolonged precipitation. Failure occurs when the maximum shear stress that the given soil can maintain is exceeded (Yalcin, 2011). Also, the friction angle decreases with increasing clay and water content in many studies (Anis et al., 2019). It is known that the volume in a soil depends heavily on the clay content. Thus, changes in water content might lead to deformation in the plastic state of the clay (Yalcin, 2011; Anis et al., 2019) and thereby might change associated mechanical properties (Meisina, 2006). In addition, plasticity increases with clay content in Flysch materials (Anis et al., 2019) and clay-rich landslides are highly susceptible to fail (Yalcin, 2011). In our study site, we can find both a highly saturated sub-surface and high clay content (most samples consist about 60 % of clay and silt fraction in other parts of the Hofermühle landslide with grain size increasing mainly with depth, see Stumvoll et al., 2022) making the area highly susceptible to future landslide events.

5. Conclusion

The Hofermühle-landslide exhibits a range of thicknesses depending on the slope surface, past alternations and previous movements. Particularly, the surface has been altered multiple times by natural creep displacement but also by human-build surface drainage channels. This might also account to the high degree of variability in resistivity when compared to the deeper layers that may be less disturbed. The findings of this study suggest that slip surfaces can be expected in the active landslide body at the surface of the bedrock. This surface is overlayed by a highly disturbed, clay-rich landslide mass without clear embedded layers or slip surfaces. Our data suggests that the geometry of the

interpreted bedrock comes closer to the recent surface in the direction of the Hofermühle torrent. Due to its higher strength, the material we interpret as bedrock hinders water infiltration wherefore water can accumulate at this boundary, especially after prolonged or heavy rainfall. In combination with the high degree of saturation in some areas, which are evident not only in the ERT profiles, but also in the presence of water puddles on the surface in the vicinity of the torrent, further movement is likely to occur – particularly triggered by future more likely and more intense rainfall events. Furthermore, ongoing surface erosion of clay along flow paths and resulting accumulation downslope can also be anticipated, reasoned by the lower resistivities and deeper mass of material (approximately 4 m) with high conductivity downslope and towards the torrent.

Having in mind the chronology of former activity reasons and extended with the results of this study, it can be concluded, that the complex Hofermühle-landslide is prone to fast earth flow or debris-flow-like events – especially in the areas where the preferential surface runoff paths are located. The most likely predisposing factor for the initiation of movement along the current slip surfaces is water infiltration following heavy and/or prolonged rainfall. ERT and DPM proved to be sufficient techniques to investigate landslide geometries and to approximate potential failure locations. These investigations provide valuable insights into landslide characteristics and subsequent dynamics, which can aid in the refinement of models and the adaption of susceptibility maps to establish effective mitigation strategies. The Flysch Zone in general is highly susceptible to landslide events due to its geology (Figdor et al., 1990; Schwenk, 1992; Schnabel, 1999; Höck et al., 2005; NOEL GV, 2008; Petschko et al., 2014; Stumvoll et al., 2020) and the detailed findings from the Hofermühle-landslide can be expected to be helpful for this whole region.

6. Perspectives

In order to determine the ongoing processes and triggering mechanisms at the Hofermühle landslide, further research is essential. In particular to estimate the exact geometries and volume of the landslide under different scenarios, more information is needed. With more data on e.g., specific material, saturation and spatial extension of slip surfaces, a detailed slope stability analysis could be conducted (Komolvilas et al., 2021), which would also provide useful information for other landslides in the larger area of the Flysch Zone in Lower Austria.

For further research on the Hofermühle landslide, a focus should therefore lie on the acquisition of borehole data, since ERT results are site-specific and cannot be generalized for all geological and geomorphological contexts (Lapenna and Perrone, 2022). A laboratory analysis of samples of the different subsurface layers could be used to match the associated materials and its properties with the collected ERT data (Merritt et al., 2014; Perrone et al., 2014). This linkage would allow better conclusions to be drawn about the depth and geometries of the landslide surfaces. Also, landslide behavior depends highly on the grain-size distribution (Yalcin, 2011, Anis et al., 2019), which could be stated with laboratory testing of soil samples from the study site. However, conditions on site have not allowed this so far. The DPM measurements have already been challenging and especially in the middle of the survey area the mass is so muddy that it is not accessible with heavy equipment. Hence, the use of electromagnetic induction (EMI) and induced polarization (IP) is advisable because they proofed to be efficient methods for studying clay-rich landslides as they allow to distinguish between saturated and clayey areas (Gallistl et al., 2018; Flores Orozco et al., 2018), which is with regards to the geology useful information in our research area.

In particular because a mud/debris flow had formed in the study area in the past after a significant rainfall event, detecting preferred (seasonal) flow paths and monitor runoff response and water accumulations after rain events are important to understand more about triggering and failure mechanisms. To achieve this aim, the implementation of time-lapse ERT (TL-ERT) as a robust and cost-effective could be used to identify, map and monitor unstable areas where failure can be expected by capturing site-specific dynamics in their seasonal variabilities (Perrone et al., 2014; Palis et al., 2017; Rezaei et al., 2018; Lapenna and Perrone, 2022). To measure the influence of parameters like prolonged and heavy rainfall, infiltration, saturation, suction and vegetation more specific, a monitoring system containing piezometers (Palis et al., 2017), a rain gauge, tensiometers, and TDR to set up a long-time multi-factor measurement (Friedel et al., 2006; Komolvilas et al., 2021).

This becomes especially important with the background of climate change, where extreme precipitation events are expected to appear more frequently (Lapenna and Perrone, 2022). Nonetheless, on-site conditions must also allow it. Permanently installed equipment could be lost within a few days in the muddy main landslide area, which is the reason why the installations at the Hofermühle landslide are not located in this area so far.

Supplementary data to this article can be found online at https://doi.org/10.1016/j.geomorph.2023.108910.

Declaration of competing interest

The authors declare that they have no known competing financial interests or personal relationships that could have appeared to influence the work reported in this paper.

Data availability

Data will be made available on request.

Acknowledgments

The authors would like to kindly thank Robert Kanta, Jakob Gallistl and Timea Katona, for their immense help and support in advance organization and during the fieldwork, as well as with the data processing. Further, we would like to sincerely thank Silke Griesser, Bastian Lindemair, Mario Schritter, Florian Vacek and Thomas Binder for their engaged assistance during the fieldwork. Additionally, a special thanks to Francisca Soto Bravo for all her great support. We are also grateful to Eduard Kotzmaier and the other WLV staff involved, as well as to the team of the Geological Survey of Lower Austria, namely Joachim Schweigl und Michael Bertagnoli and of course the landowners, especially Johannes Oberbramberger, for letting us conduct our measurements on their ground.

References

Akingboye, A.S., Ogunyele, A.C., 2019. Insight into seismic refraction and electrical resistivity tomography techniques in subsurface investigations. The Mining-Geology-Petroleum Engineering Bulletin 93–111. https://doi.org/10.17794/rgn.2019.1.9.

Anis, Z., Wissem, G., Riheb, H., Biswajeet, P., Essghaier, G.M., 2019. Effects of clay properties in the landslides genesis in flysch massif: Case study of Aïn Draham, North Western Tunisia. J. Afr. Earth Sci. 151, 146–152. https://doi.org/10.1016/j.jafrearsci.2018.12.005.

Asriza, S., Kristyanto, T.H.W., Indra, T.L., Syahputra, R., Tempessy, A.S., 2017. Determination of the landslide slip surface using electrical resistivity tomography (ERT) technique, 2017. In: Mikos, et al. (Eds.), Advancing Culture of Living with Landslides. Springer International Publishing AG, pp. 53–60. https://doi.org/10.1007/978-3-319-53498-5_7.

Auer, I., Böhm, R., Jurkovic, A., Lipa, W., Orlik, A., Potzmann, R., Schöner, W., Ungersböck, M., Matulla, C., Briffa, K., Jones, P., Efthymiadis, D., Brunetti, M., Nanni, T., Maugeri, M., Mercalli, L., Mestre, O., Moisselin, J.-M., Begert, M., Müller-Westermeier, G., Kveton, V., Bochnicek, O., Stastny, P., Lapin, M., Szalai, S., Szentimrey, T., Cegnar, T., Dolinar, M., Gajic-Capka, M., Zaninovic, K., Majstorovicp, Z., Nieplova, E., 2007. HISTALP – historical instrumental climatological surface time series of the Greater Alpine Region. In: Int. J. Climatol. 27, 17–46. https://doi.org/10.1002/joc.1.

Avanzi, G. D'Amato, Galanti, Y., Giannecchini, R., Duchi, S., Lo Presti, D., Marchetti, D., 2013a. DP test in geotechnical characterization of shallow landslides source area: results and perspectives. Landslide Science and Practice: Landslide Inventory and Susceptibility and Hazards Zoning1 249–255. https://doi.org/10.1007/978-3-642-31325-7_33.

Avanzi, G. D'Amato, Galanti, Y., Giannecchini, R., Lo Presti, D., Puccinelli, A., 2013b. Estimation of soil properties of shallow landslide source areas by dynamic penetration tests: first outcomes from Northern Tuscany (Italy). Bull. Eng. Geol. Environ. 72, 609–624. https://doi.org/10.1007/s10064-013-0535-y.

Bell, R., 2007. Lokale und regionale Gefahren- und Risikoanalyse gravitativer Massenbewegungen an der Schwäbischen Alb. Rheinische Friedrich-Wilhelms-Universität Bonn, Bonn.

Bell, R., Kruse, J.E., Garcia, A., Glade, T., Hördt, A., 2006. Subsurface investigations of landslides using geophysical methods – geoelectrical applications in the Swabian Alb (Germany). Geographica Helvetica 201–208.

Bell, R., Glade, T., Granica, K., Heiss, G., Leopold, P., Petschko, H., Pomaroli, G., Proske, H., Schweigl, J., 2011. Landslide susceptibility maps for spatial planning in Lower Austria. In: Proceedings of the Second World Landslide Forum – 3-7 October 2011, Rome, pp. 1–6.

Binley, A. and Kemna, A. (2005): DC resistivity and induced polarization methods. In: Rubin, Y. and Sharpesshubbard, S. (Edt.) (2005): Hydrogeophysics: 129–156. DOI: https://doi.org/10.1007/1-4020-3102-5_5.

BML, 2023. Ehyd Web GIS Application. Internet. https://ehyd.gv.at/#.

Crozier, M.J., Glade, T., 2005. Landslide Hazard and risk: Issues, Concepts and Approach. In: Glade, T., Anderson, M.G., Crozier, M.J. (Eds.), Landslide Risk Assessment. John Wiley, New York, pp. 1–40. https://doi.org/10.1002/9780470012659.ch1.

Cruden, D.M., Varnes, D.J., 1996. Landslide types and processes. In: Turner, A.K., Schuster, R.L. (Eds.), Landslides Investigation and Mitigation. Transportation Research Board, US National Research Council. Special Report, 247, pp. 36–75.

Dikau, R., Brunsden, D., Schrott, L. (Eds.), 1996. Landslide Recognition. Identification, Movement and Causes.

Ehrlich, D., Melchiorri, M., Capitani, C., 2021. Population Trends and Urbanisation in Mountain Ranges of the World. In: Land 10 (255), 1–18. https://doi.org/10.3390/land10030255.

Falae, P.O., Kanungo, D.P., Chauhan, P.K.S., Dash, R.K., 2019. Electrical resistivity tomography (ERT) based subsurface characterisation of Pakhi Landslide, Garhwal Himalayas, India. In. Environ. Earth Sci. 78 (430), 1–18. https://doi.org/10.1007/s12665-019-8430-x.

Figdor, H., Roch, K.-H., Scheidegger, A.E., 1990. Geophysikalische und geodätische Untersuchungen an einer Hangrutschung im Flysch. Österreichische Zeitschrift für Vermessungswesen und Photogrammetrie 78 (4), 212–220.

Flores Orozco, A., Kemna, A., Zimmermann, E., 2012. Data error quantification in spectral induced polarization imaging. In: Geophysics 77 (3), E227–E237.

Flores Orozco, A., Williams, K.H., Kemna, A., 2013. Time-lapse spectral induced polarization imaging of stimulated uranium bioremediation. Near Surface Geophysics 11 (5), 531–544.

Flores Orozco, A., Bücker, M., Steiner, M., Malet, J.-P., 2018. Complex-conductivity imaging for the understanding of landslide architecture. Engineering Geology 243, 241–252. https://doi.org/10.1016/j.enggeo.2018.07.009.

Flores Orozco, A., Steiner, M., Katona, T., Roser, N., Moser, C., Stumvoll, M.J., Glade, T., 2022. Application of induced polarization imaging across different scales to understand surface and groundwater flow at the Hofermuehle landslide. Catena 219, 1–18. https://doi.org/10.1016/j.catena.2022.106612.

Friedel, S., Thielen, A., Springman, S.M., 2006. Investigation of a slope endangered by rainfall-induced landslides using 3D resistivity tomography and geotechnical testing. J. Appl. Geophys. 60 (2), 100–114. https://doi.org/10.1016/j.jappgeo.2006.01.001.

Gallistl, J., Weigand, M., Stumvoll, M., Ottowitz, D., Glade, T., Orozco, A.F., 2018. Delineation of subsurface variability in clay-rich landslides through spectral induced polarization imaging and electromagnetic methods. Engineering Geology 245, 292–308. https://doi.org/10.1016/j.enggeo.2018.09.001.

Glade, T., Petschko, H., Bell, R., Bauer, C., Granica, K., Heiss, G., Leopold, P., Pomaroli, G., Proske, H. and Schweigl, J. (2012): Landslide susceptibility maps for Lower Austria. Methods and challenges. 12th Congress INTERPRAEVENT 2012 - Grenoble/France, Conference Proceedings: 497–508.

Goetz, J.N., Cabrera, R., Brenning, A., Heiss, G., Leopold, P., 2015. Modelling Landslide Susceptibility for a large Geographical Area using Weights of evidence in Lower Austria, Austria. In Engineering Geology for Society and Territory 2, 927–930. https://doi.org/10.1007/978-3-319-09057-3_160.

González-Álvarez, I., Ley-Cooper, A.-Y., Salama, W., 2016. A geological assessment of airborne electromagnetics for mineral exploration through deeply weathered profiles in the southeast yilgarn cratonic margin, Western Australia. Ore Geol. Rev. 73, 522–539. https://doi.org/10.1016/j.oregeorev.2015.10.029.

Höck, V., Slaczka, A., Gasinski, M.A., Bak, M., 2005. Konradsheim limestone of the Gresten Klippen Zone (Austria): new insight into its stratigraphic and paleogeographic setting. Geologica Carpathica 56, 237–244.

Hungr, O., Leroueil, S., Picarelli, L., 2013. The Varnes classification of landslide types, an update. Landslides 11 (2), 167–194. https://doi.org/10.1007/s10346-013-0436-y.

Imani, P., Tian, G., Hadiloo, S., El-Raouf, A.A., 2021. Application of combined electrical resistivity tomography (ERT) and seismic refraction tomography (SRT) methods to investigate Xiaoshan District landslide site: Hangzhou, China. Journal of Applied Geophysics 184, 1–13. https://doi.org/10.1016/j.jappgeo.2020.104236.

Jaesche, P., Huwe, B., Stingl, H., Veit, H., 2002. Temporal Variability of Alpine Solifluction: a modelling approach. In: Geographica Helvetica Jg. 57. Heft 3, 157–169.

Kaminski, M., Zientara, P., Krawczyk, M., 2021. Electrical resistivity tomography and digital aerial photogrammetry in the research of the "Bachledzki Hill" active landslide – in Podhale (Poland). Eng. Geol. 285, 1–17. https://doi.org/10.1016/j.enggeo.2021.106004.

Kemna, A. (2000): Tomographic Inversion of Complex Resistivity—Theory and Application. Der Andere Verlag, Osnabrück. Ausgabe 56 von Berichte des Instituts für Geophysik der Ruhr-Universität Bochum/A, Ruhr-Universität Bochum Institut für Geophysik: 1–176.

Khan, M.A., Basharat, M., Riaz, M.T., Sarfraz, Y., Farooq, M., Khan, A.Y., Pham, Q.B., Ahmed, K.S., Shahzad, A., 2021. An integrated geotechnical and geophysical investigation of a catastrophic landslide in the Northeast Himalayas of Pakistan. Geol. J. 56, 4760–4778. https://doi.org/10.1002/gj.4209.

Komolvilas, V., Tanapalungkorn, W., Latcharote, P., Likitlersuang, S., 2021. Failure analysis on a heavy rainfall-induced landslide in Huay Khab Mountain in Northern Thailand. Journal of Mountain Science 18 (10), 2580–2596. https://doi.org/10.1007/s11629-021-6720-8.

Kotzmaier, E. (2013): Aktenvermerk Krojer Rutschung (Hofermühle) 03.05.2013, Wildbach und Lawinenverbauung Niederösterreich West, Melk, Austria.

Lapenna, V., Perrone, A., 2022. Time-lapse electrical resistivity tomography (TL-ERT) for landslide monitoring: recent advances and future directions. Applied Sciences 12 (1425), 1–16. https://doi.org/10.3390/app12031425, 2022.

Li, X., Handwerger, A.L., Buscarnera, G., 2023. Viscoplastic modelling of rainfall-drivenslow-moving landslides: application to California Coast Ranges. Landslides. https://doi.org/10.1007/s10346-023-02039-1, 1–14 Feb. 2023.

Liebetruth, F. (2014): Sondierungen und deren Bewertung. 65. Deutsche Brunnenbauertage und BAW Baugrundkolloquium, 7.9. Mai im Bau ABS Rostrup/Bad Zwischenahn: 53-59.

Lima, P., Steger, S., Glade, T., Tilch, N., Schwarz, L., Kociu, A., 2017. Landslide susceptibility mapping at national scale: a first attempt for Austria. In: Mikoš, M., Tiwari, B., Yin, Y., Sassa, K. (Eds.), Advancing Culture of Living with Landslides, pp. 943–951. https://doi.org/10.1007/978-3-319-53498-5_107.

Mantovani, M., Bossi, G., Dykes, A.P., Pasuto, A., Soldati, M., Devoto, S., 2022. Coupling long-term GNSS monitoring and numerical modelling of lateral spreading for hazard assessment purposes. Engineering Geology 29, 1–14. https://doi.org/10.1016/j.enggeo.2021.106466.

Marr, P., Donato, A. J., Carraro, E., Kanta, R. and Glade, T. (2023): The role of historical data to investigate slow-moving landslides by long-term monitoring systems in Lower Austria. In: Land 2023, 11, x.: 1-22. doi:https://doi.org/10.3390/xxxxx.

Meisina, C., 2006. Characterisation of weathered clayey soils responsible for shallow landslides. Nat. Hazards Earth Syst. Sci. 6, 825–838. https://doi.org/10.5194/nhess-6-825-2006.

Merritt, A.J., Chambers, J.E., Murphy, W., Wilkinson, P.B., West, L.J., Gunn, D.A., Meldrum, P.I., Kirkham, M., Dixon, N., 2014. 3D ground model development for an active landslide in Lias mudrocks using geophysical, remote sensing and geotechnical methods. Landslides 11, 537–550. https://doi.org/10.1007/s10346-013-0409-1.

NOEL Gv (Amt der Niederösterreichischen Landesregierung) (2008): Waldentwicklungsplan –Teilplan über den Bereich des politischen Bezirkes Amstetten und der Statutarstadt Waidhofen/Ybbs (2. Revision): 1–219.

Palis, E., Lebourg, T., Vidal, M., Levy, C., Tric, E., Hernandez, M., 2017. Multiyear time-lapse ERT to study short- and long-term landslide hydrological dynamics. Landslides 14, 1333–1343. https://doi.org/10.1007/s10346-016-0791-6.

Perrone, A., Lapenna, V., Piscitelli, S., 2014. Electrical resistivity tomography technique for landslide investigation: A review. Earth Sci. Rev. 135, 65–82. https://doi.org/10.1016/j.earscirev.2014.04.002.

Petschko, H., Bell, R., Leopold, P., Heiss, G., Glade, T., 2013. Landslide inventories for Reliable Susceptibility Maps in Lower Austria. In: Margottini, C., Canuti, P., Sassa, K. (Eds.), Landslide Science and Practice. Springer, Berlin, Heidelberg. https://doi.org/10.1007/978-3-642-31325-7_37.

Petschko, H., Brenning, A., Bell, R., Goetz, J., Glade, T., 2014. Assessing the quality of landslide susceptibility maps – case study Lower Austria. Nat. Hazards Earth Syst. Sci. 14, 95–118. https://doi.org/10.5194/nhess-14-95-2014.

Picarelli, L., 2007. Considerations about the Mechanics of Slow active Landslides in Clay. In: Sassa, K., Fukuoka, H., Wang, F., Wang, G. (Eds.), Progress in Landslide Science. Springer, Berlin, Heidelberg, pp. 27–45. https://doi.org/10.1007/978-3-540-70965-7_3.

Revil, A., Ahmed, A.S., Coperey, A., Ravanel, L., Sharma, R., Panwar, N., 2020. Induced polarization as a tool to characterize shallow landslides. J. Hydrol. 589 (125369), 1–12. https://doi.org/10.1016/j.jhydrol.2020.125369.

Rezaei, S., Shooshpasha, I., Rezael, H., 2018. Reconstruction of landslide model from ERT, geotechnical, and field data, Nargeschal landslide, Iran. Bulletin of Engineering Geology and the Environment 1–15. https://doi.org/10.1007/s10064-018-1352-0.

Samodra, G., Ramadhan, M.F., Sartohadi, J., Setiawan, M.A., Christanto, N., Sukmawijaya, A., 2020. Characterization of displacement and internal structure of landslides from multitemporal UAV and ERT imaging. Landslides 17, 2455–2468. https://doi.org/10.1007/s10346-020-01428-0.

Sass, O., Bell, R., Glade, T., 2008. Comparison of GPR, 2D-resistivity and traditional techniques for the subsurface exploration of the Öschingenlandslide, Swabian Alb (Germany). Geomorphology 93, 89–103. https://doi.org/10.1016/j.geomorph.2006.12.019.

Sausgruber, T. (2013): Hofermühlrutschung Waidhofen/Ybbs (intern). Mit zwei Anhängen (Kartierung), Forsttechnischer Dienst für Wildbach und Lawinenverbauung. Geologische Stelle, Innsbruck, Austria.

Sausgruber, T. (2016): Protokoll zum Lokalaugenschein Hangprozess Hofermühle/Hofermühlrutschung, am 11.10.2016. Forsttechnischer Dienst für Wildbach und Lawinenverbauung. Geologische Stelle, Innsbruck, Austria, Mit einem Anhang (Kartierung).

Scapozza, C., Laigre, L., 2014. The contribution of Electrical Resistivity Tomography (ERT) in Alpine dynamics geomorphology: case studies from the Swiss Alps. Géomorphologie 20 (1), 27–42. https://doi.org/10.4000/geomorphologie.10474.

Schnabel, W. (1999): The Flysch Zone of the Eastern alps vol. 49. Verlag der Geologischen Bundesanstalt (GBA). Wien.

Schnabel, W. (2002): Geologische Karte von Niederösterreich 1:200.000. Geologische Bundesanstalt, Wien, Österreich.
Schwenk, H. (1992): Massenbewegungen in Niederösterreich 1953–1990. In: Jb. Geol. B.-A, Band 135, Heft 2: 597–660.
Shah, N.A., Shafique, M., Ishfaq, M., Faisal, K., Van der Meijde, M., 2023. Integrated approach for landslide risk assessment using geoinformation tools and field data in Hindukush Mountain Ranges, Northern Pakistan. Sustainability 2023 15 (3102), 1–23. https://doi.org/10.3390/su15043102.
Soto, J., Galve, J.P., Palenzuela, J.A., Azañón, J.M., Tamay, J., Irigaray, C., 2017. A multi-method approach for the characterization of landslides in an intramontane basin in the Andes (Loja, Ecuador). In: Landslides. https://doi.org/10.1007/s10346-017-0830-y.
Steger, S., Schmaltz, E., Seijmonsbergen, A.C., Glade, T., 2022. The Walgau: A Landscape shaped by Landslides. In: Embleton-Hamann, C. (Ed.), Landscapes and Landforms of Austria. World Geomorphological Landscapes. Springer, Cham. https://doi.org/10.1007/978-3-030-92815-5_15.
Stumvoll, M.J., Canli, E., Engels, A., Thiebes, B., Glade, T., Schweigl, J., Bertagnoli, M., 2020. The "Salcher"landslide observatory—experimental long-term monitoring in the Flysch Zone of Lower Austria. Bulletin of Engineering Geology and the Environment 79, 1831–1848. https://doi.org/10.1007/s10064-019-01632-w.
Stumvoll, M.J., Schmaltz, E.M., Glade, T., 2021. Dynamic characterization of a slow-moving landslide system – Assessing the challenges of small process scales utilizing multi-temporal TLS data. Geomorphology 389, 1–16. https://doi.org/10.1016/j.geomorph.2021.107803.
Stumvoll, M.J., Schmaltz, E.M., Kanta, R., Roth, H., Grall, B., Luhn, J., Flores-Orozco, A., Glade, T., 2022. Exploring the dynamics of a complex, slow-moving landslide in the Austrian Flysch Zone with 4D surface and subsurface information. Catena 214, 1–15. https://doi.org/10.1016/j.catena.2022.106203.
Terhorst, B., Damm, B., 2009. Slope Stability and Slope Formation in the Flysch Zone of the Vienna Forest (Austria). Journal of Geological Research 2009, 1–10. https://doi.org/10.1155/2009/589037.
Thenius, E., 1974. Geologie der österreichischen Bundesländer in kurzgefassten Einzeldarstellungen. Niederösterreich, Geologische Bundesanstalt, Wien, Österreich, pp. 85–109.
University of Vienna - NoeSLIDE, 2022. Internet. https://www.noeslide.at/index.php/de/hofermuehle.
Veit, H. (2002): Relict soils as paleoclimatic indicators: examples from the Austrian Alps and the Central Andes. Presentation at 17 th WCSS, 14–21 August 2002, Thailand. Symposium no. 49, Paper no. 182: 1–11.
Weigand, M., Flores Orozco, A., Kemna, A., 2017. Reconstruction quality of SIP parameters in multi-frequency complex resistivity imaging. Near Surface Geophysics 15 (2), 187–199.
Wenner, F. (1915): A Method of Measuring Earth Resistivity. In: The Bulletin of the Bureau of Standards 12, Scientific Paper no. 258: 469–478.
Whiteley, J.S., Chambers, J.E., Uhlemann, S., Wilkinson, P.B., Kendall, J.M., 2019. Geophysical monitoring of moisture-induced landslides: A review. Rev. Geophys. 57, 106–145. https://doi.org/10.1029/2018RG000603.
Yalcin, A., 2011. A geotechnical study on the landslides in the Trabzon Province, NE, Turkey. Appl. Clay Sci. 52, 11–19. https://doi.org/10.1016/j.clay.2011.01.015.
Yin, Y., Li, B., Wang, W., Zhan, L., Xue, Q., Gao, Y., Zhang, N., Chen, H., Liu, T., Li, A., 2016. Mechanism of the December 2015 catastrophic landslide at the Shenzhen landfill and controlling geotechnical risks of urbanization. Engineering 2, 230–249. https://doi.org/10.1016/J.ENG.2016.02.005.